Orientational order in model dipolar fluids

Philip J. Camp and G. N. Patey
Department of Chemistry, University of British Columbia, Vancouver, Canada V6T 1Z1
(Received 12 April 1999)

Fluids of hard spheres each carrying two parallel point dipoles have been investigated using constant-volume Monte Carlo computer simulations. The results show that both ferroelectric and antiferroelectric fluid phases can be stabilized at high density and low temperature by dipolar interactions alone, if the separation between the dipoles on each sphere is sufficiently large. A simple lattice calculation provides some insight into the balance between dipole energy and orientational entropy which governs the polarization state.
[S1063-651X(99)00610-8]

PACS number(s): 61.20.Ja, 64.70.Md, 75.50.Mm, 77.80.−e

I. INTRODUCTION

In a ferroelectric phase of dipolar molecules the orientations of the molecular dipoles are aligned so as to give a net macroscopic dipole moment. Born was the first to consider whether orientational order could be induced in the fluid phase by dipole-dipole interactions alone [1], but this issue remained largely unanswered until recently. While ferroelectric fluids have proved elusive in the laboratory, computer simulations [2–4] and theoretical studies [5,6] have identified molecular models which do exhibit such phases. Computer simulations have shown that dense fluids and solids made up of point dipolar soft spheres exhibit ferroelectric phases at sufficiently low temperatures [2], as have simulations of the corresponding dipolar hard-sphere model [3,4]. It is a combination of the long-range interactions between the aligned dipoles and the resulting reaction field, and short-range correlations which stabilizes the ferroelectric state. As a result, while simulations using conducting boundary conditions result in a ferroelectric phase, those using vacuum boundary conditions result in a domain structure with no net polarization [2].

Antiferroelectric orientationally ordered phases have also been observed in simulations of nonspherical dipolar hard particles using conducting boundary conditions [7]. These phases are stabilized by the anisotropy of the short-range repulsions, i.e., the shape of the molecules, as well as by the long-range electrostatic interactions. In this paper we present evidence from computer simulations of a homogeneous antiferroelectric orientationally ordered phase formed by a fluid of hard spheres carrying two point dipoles. The fluid possesses $\hat{\mathbf{n}} \leftrightarrow -\hat{\mathbf{n}}$ symmetry, where $\hat{\mathbf{n}}$ is the preferred direction of alignment, or director. Such a fluid can therefore be described as having normal nematic order, as this symmetry is also present in nematic liquid crystals. Since the short-range repulsions are isotropic, the antiferroelectric phase is stabilized solely by the electrostatic interactions. The particle model we consider is sketched in Fig. 1. It consists of a hard sphere of diameter σ, possessing two parallel point dipoles, $\boldsymbol{\mu}_1 = \boldsymbol{\mu}_2 = \mu\hat{\mathbf{e}}$, where μ is the dipole moment and $\hat{\mathbf{e}}$ is the unit orientation vector. $\boldsymbol{\mu}_1$ and $\boldsymbol{\mu}_2$ are displaced from the sphere center by $\pm(\kappa\sigma/2)\hat{\mathbf{e}}$. The interaction energy between two such spheres is given by the hard-core interaction plus a sum over the interactions between dipoles on different spheres. The interaction energy u_{ij}^{DD} between two dipoles $\boldsymbol{\mu}_i$ and $\boldsymbol{\mu}_j$, with position vectors $\mathbf{r}_i$ and $\mathbf{r}_j$, respectively, is

$$u_{ij}^{\mathrm{DD}} = \frac{\boldsymbol{\mu}_i \cdot \boldsymbol{\mu}_j}{r_{ij}^3} - \frac{3(\boldsymbol{\mu}_i \cdot \mathbf{r}_{ij})(\boldsymbol{\mu}_j \cdot \mathbf{r}_{ij})}{r_{ij}^5}, \tag{1}$$

where $\mathbf{r}_{ij} = \mathbf{r}_j - \mathbf{r}_i$ and $r_{ij} = |\mathbf{r}_{ij}|$. This model is an extension of the normal dipolar hard-sphere model, where the central dipole is split in half and the moieties displaced towards the edge of the sphere. Although these dipolar hard-sphere models may not be particularly realistic for molecules, they do have some relevance for ferrofluids and colloidal suspensions [8–10]. Furthermore, by selecting a spherical hard-core interaction we are able to isolate dipolar effects explicitly.

The system is characterized by the following quantities. The reduced number density is $\rho^* = \rho\sigma^3$, where $\rho = N_s/V$, N_s is the number of spheres, and V is the volume of the cubic simulation cell. The reduced dipole moment is given by $\mu^* = \sqrt{\mu^2/k_B T\sigma^3}$, where k_B is Boltzmann's constant and T is the temperature. In the simulations $\mu^* = 1.25$, so that the total dipole moment on each sphere $\mu^*_{\mathrm{total}} = 2.5$. The reduced temperature is given by $T^* = (1/\mu^*)^2 = 0.64$. A dipole separation of $\kappa\sigma = 0$ corresponds to the normal dipolar hard-sphere system in which Weis and Levesque found ferroelectric fluid and ferroelectric solid phases [3,4]. Weis and Levesque report a ferroelectric phase for $\mu^*_{\mathrm{total}} = 2.5$ when $\rho^* \geqslant 0.80$, and for $\mu^*_{\mathrm{total}} = 3.5$ when $\rho^* \geqslant 0.30$.

This paper is organized as follows. In Sec. II we provide details of the simulation method used in this study. In Sec. III we present the simulation results. In Sec. IV we describe

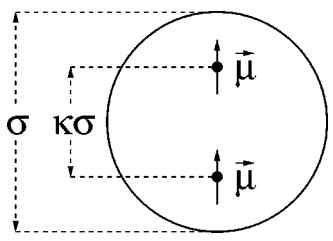

FIG. 1. Sketch of the dipolar hard-sphere model. The dipoles are of equal magnitude, parallel and equidistant from the center of the sphere.

a simple lattice calculation which helps in the interpretation of the simulation results. Section V concludes the paper.

II. COMPUTER SIMULATIONS

We have performed constant-volume Monte Carlo (MC) simulations of $N_s=125$ or 256 spheres with dipole separations $\kappa\sigma=0$, 0.25σ, and 0.3σ. For each dipole separation and system size, we have studied densities in the range $0.4 \leqslant \rho^* \leqslant 0.925$. All simulations were performed using cubic periodic boundary conditions. The long-range dipolar interactions were handled using the Ewald summation method [11,12], with conducting boundary conditions (the dielectric constant of the surrounding continuum $\epsilon'=\infty$). All dipole-dipole interactions were included in the energy sum except those between dipoles on the same sphere. In *every* simulation the initial configuration was that of a well-equilibrated hard-sphere fluid with random dipole orientations chosen uniformly from the unit sphere. Each MC cycle consisted of an attempted translation and rotation of N_s randomly selected particles. The displacement parameters were adjusted to give approximately 30% acceptance rates for both translations and rotations. A typical run consisted of at least 10^5 MC cycles for equilibration followed by at least another 10^5 MC cycles over which block averages were accumulated. Equilibrium quantities were calculated every 10 MC cycles, and averaged over blocks of 10^3 MC cycles. Statistical errors were estimated by treating each block average as a statistically independent measurement.

Orientational order was monitored by calculating the second-rank order tensor $\mathbf{Q}$, defined by [13]

$$\mathbf{Q}=\frac{1}{2N_s}\sum_{i=1}^{N_s}(3\hat{\mathbf{e}}_i\hat{\mathbf{e}}_i-\mathbf{I}), \tag{2}$$

where $\hat{\mathbf{e}}_i$ is the orientation unit vector of sphere i and $\mathbf{I}$ is the second-rank unit tensor. Diagonalization of $\mathbf{Q}$ yields three eigenvalues and three eigenvectors. The highest eigenvalue is the second-rank order parameter S, and the corresponding normalized eigenvector is the director $\hat{\mathbf{n}}$ [14]. S can also be expressed as the average of $(3\cos^2\theta-1)/2$ over all of the particles, where θ is the angle between the orientation vector of a given particle and the instantaneous director. S is unity in perfectly aligned ferroelectric and antiferroelectric phases and zero in the isotropic phase. The polarization P is given by

$$P=\left|\frac{1}{N_s}\sum_{i=1}^{N_s}\hat{\mathbf{e}}_i\cdot\hat{\mathbf{n}}\right|. \tag{3}$$

P is unity in a perfectly aligned ferroelectric phase and zero in an antiferroelectric phase and in the isotropic phase. S is therefore the indicator of orientational order and P discriminates between ferroelectric and antiferroelectric phases. In a ferroelectric phase $P\simeq\sqrt{(2S+1)/3}\geqslant S$, while in an antiferroelectric phase $P<S$. Using these criteria a ferroelectric phase can be distinguished from an antiferroelectric phase. Finite-size effects are apparent in S calculated via the diagonalization of $\mathbf{Q}$ [15]; in the isotropic fluid the errors are $\mathcal{O}(1/\sqrt{N_s})$, while in orientationally ordered phases they are $\mathcal{O}(1/N_s)$.

TABLE I. MC simulation results with dipole separation $\kappa\sigma$ and reduced density ρ^*. U is the average configurational energy, P is the polarization, and S is the second-rank order parameter. The numbers in parentheses denote the statistical uncertainty in the last digit.

ρ^*	$U\sigma^3/N_s\mu^2$	P	S	MC cycles/10^3
		$\kappa=0,\ N_s=125$		
0.40	−7.1(1)	0.25(6)	0.12(4)	200
0.50	−7.21(8)	0.4(1)	0.14(5)	236
0.60	−7.36(7)	0.3(1)	0.13(3)	226
0.70	−7.72(5)	0.68(7)	0.36(8)	264
0.80	−8.05(7)	0.76(3)	0.46(5)	300
0.90	−8.41(5)	0.82(1)	0.57(3)	365
		$\kappa=0.25,\ N_s=125$		
0.40	−8.54(8)	0.07(2)	0.08(2)	200
0.50	−8.56(8)	0.31(1)	0.25(1)	324
0.60	−8.4(1)	0.63(3)	0.34(4)	339
0.70	−8.81(7)	0.902(5)	0.74(1)	340
0.80	−8.97(7)	0.932(7)	0.81(2)	400
0.90	−9.01(6)	0.946(2)	0.850(6)	400
		$\kappa=0.3,\ N_s=125$		
0.40	−9.59(7)	0.26(4)	0.09(1)	200
0.50	−9.56(6)	0.09(1)	0.26(1)	180
0.60	−9.46(7)	0.19(1)	0.17(1)	400
0.70	−9.42(8)	0.10(4)	0.16(1)	400
0.80	−9.38(6)	0.09(1)	0.34(2)	400
0.90	−9.66(6)	0.207(4)	0.546(7)	400
		$\kappa=0.3,\ N_s=256$		
0.40	−9.64(5)	0.082(6)	0.13(1)	33
0.50	−9.59(4)	0.085(7)	0.090(7)	56
0.60	−9.61(3)	0.14(1)	0.12(1)	76
0.70	−9.70(5)	0.021(4)	0.133(6)	397
0.80	−9.80(5)	0.17(2)	0.153(9)	445
0.90	−9.86(3)	0.138(4)	0.444(6)	414
0.925[a]	−10.09(4)	0.63(1)	0.61(1)	1000
0.925[b]	−10.15(6)	0.20(1)	0.61(1)	797

[a]Run 1.
[b]Run 2.

III. RESULTS

A. $\kappa=0$

In Table I we report simulation results for $\kappa=0$ and $N_s=125$. With a dipole moment $\mu^*=1.25$ this system corresponds to the normal dipolar hard-sphere fluid with $\mu^*_{\text{total}}=2.5$ as simulated by Weis and Levesque [3]. Our results for the energies and order parameters agree well with the data in Ref. [3]. In Fig. 2 we show the order parameters P and S against density. Our results confirm the existence of a ferroelectric phase ($S>0$, $P>S$) at densities $\rho^*\geqslant 0.7$. As noted in Sec. II, in the isotropic phase finite-size effects account for nonzero order parameters which are $\mathcal{O}(10^{-1})$.

B. $\kappa=0.25$

In Table I we list simulation results for $\kappa=0.25$ and $N_s=125$. In Fig. 3 we show the order parameters P and S against density. It is clear that a ferroelectric phase (characterized by $S>0$ and $P\geqslant S$) appears at a density $\rho^*\simeq 0.6$. At

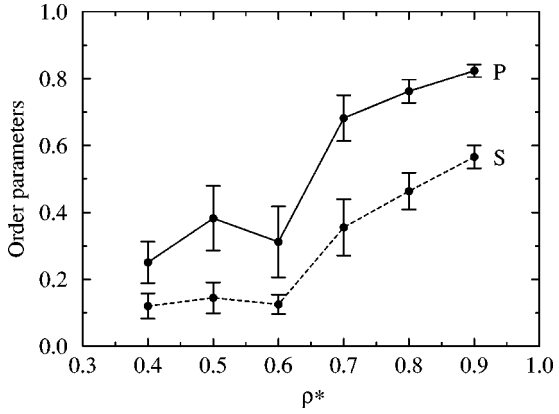

FIG. 2. Order parameters against reduced density ρ^* for $\kappa=0$, $N_s=125$: polarization P (solid line); second-rank order parameter S (dashed line).

a density $\rho^*=0.9$, the order parameters attain equilibrium values of $P\simeq 0.95$ and $S\simeq 0.85$, which are to be compared with $P\simeq 0.82$ and $S\simeq 0.57$ for $\kappa=0$ at the same density. The increase in the orientational order and the decrease in the transition density on changing from $\kappa=0$ to $\kappa=0.25$ are likely due to the lowering of the energy associated with the nose-to-tail configuration of the spheres. This results in an increase in orientational correlations which eventually give way to global orientational order as the associated correlation length diverges. With a dipole separation of $\kappa\sigma=0.25\sigma$ the system still favors ferroelectric order at high density; we shall discuss this point further in Sec. IV.

The relative scarcity of ferroelectric liquids in the laboratory is likely due to the fact that crystallization often preempts the isotropic-ferroelectric-liquid transition. To check that the system is fluid we have monitored the ''diffusion'' of particles by calculating the mean-squared displacement as follows:

$$\langle R^2\rangle_\tau=\frac{1}{N_s}\sum_{i=1}^{N_s}[\mathbf{r}_i(\tau)-\mathbf{r}_i(0)]^2, \tag{4}$$

where $\mathbf{r}_i(0)$ is the position of the ith particle at the start of the simulation, and $\mathbf{r}_i(\tau)$ is its position after τ MC cycles.

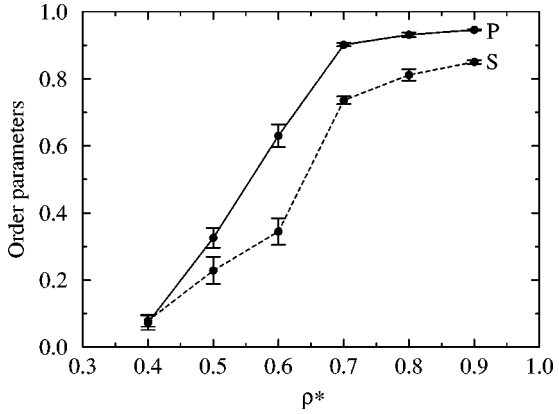

FIG. 3. Order parameters against reduced density ρ^*, for $\kappa=0.25$, $N_s=125$: polarization P (solid line); second-rank order parameter S (dashed line).

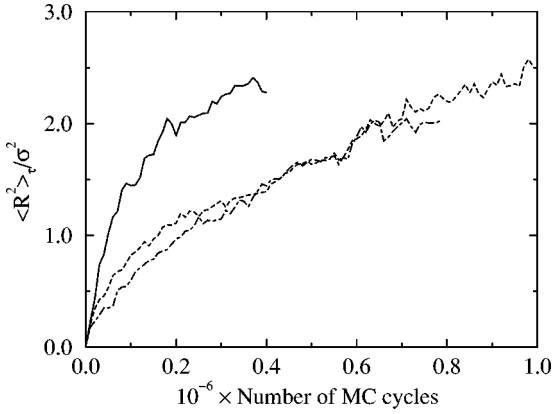

FIG. 4. Mean-squared displacement $\langle R^2\rangle_\tau$ against Monte Carlo cycle: $\kappa=0.25$, $\rho^*=0.9$, and $N_s=125$ (solid line); $\kappa=0.3$, $\rho^*=0.925$, and $N_s=256$, run 1 (dashed line) and run 2 (dot-dashed line).

For the calculation of $\langle R^2\rangle_\tau$ the particles were allowed to leave the central simulation cell. In Fig. 4 we show the evolution of $\langle R^2\rangle_\tau$ during simulations with $\kappa=0.25$ at a density $\rho^*=0.9$, i.e., the highest density studied with this dipole separation. Clearly the particles are diffusing at this high density and hence the system is fluid. We conclude, therefore, that the system with $\kappa=0.25$ undergoes a transition to a ferroelectric fluid at high density.

C. $\kappa=0.3$

Simulation results for $\kappa=0.3$ and system sizes $N_s=125$ and $N_s=256$ are given in Table I. With this dipole separation we find strong second-rank orientational order ($S>0$) for all runs with $\rho^*\geqslant 0.9$. In this density regime three simulations showed antiferroelectric order ($N_s=125$, $\rho^*=0.9$; $N_s=256$, $\rho^*=0.9$; $N_s=256$, $\rho^*=0.925$, run 2) and one showed ferroelectric order ($N_s=256$, $\rho^*=0.925$, run 1). Runs 1 and 2 with $N_s=256$ and $\rho^*=0.925$ were started from different well-equilibrated hard-sphere configurations. Table I shows that the configurational energies in the ferroelectric and antiferroelectric states in runs 1 and 2 are identical within statistical accuracy, as are the second-rank order parameters. Clearly there is no longer a strong preference to be in a ferroelectric state over an antiferroelectric state. Inspection of some simulation configurations confirmed that the antiferroelectric states for each system size were homogeneous and free of the ferroelectric domains which have been observed in simulations of dipolar particles in vacuum boundary conditions ($\epsilon'=1$) [2].

In Fig. 5 we show the evolution of the order parameters during runs 1 and 2 with $\kappa=0.3$ and $\rho^*=0.925$. In both cases very long runs were required, which reflects the sampling difficulties which arise from the strong dipole-dipole attraction between spheres in the nose-to-tail configuration.

In Fig. 4 we include $\langle R^2\rangle_\tau$ for runs 1 and 2. It is clear that the systems are fluid. After 10^6 MC sweeps each particle, on average, has diffused approximately one-and-a-half sphere diameters, which highlights the difficulty in simulating systems with strong highly directional attractive potentials. It is these sampling difficulties which precluded us from simulating systems with $\kappa>0.3$; some preliminary runs with κ

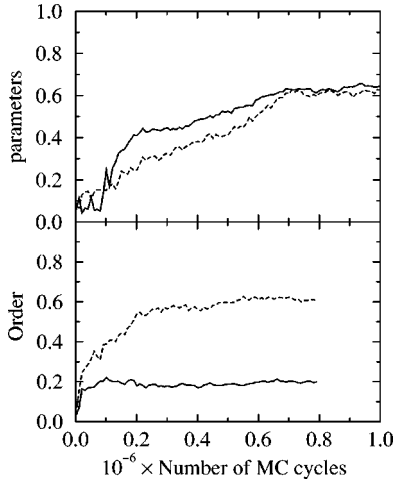

FIG. 5. Evolution of the order parameters during the two simulations with $\kappa=0.3$, $\rho^*=0.925$, and $N_s=256$: run 1 (top); run 2 (bottom); P (solid line); S (dashed line).

$=0.35$ and $\kappa=0.5$ showed very sluggish behavior and did not converge within accessible run lengths.

IV. LATTICE CALCULATION

The simulation results reported in Sec. III can be summarized as follows. For $\kappa=0$, 0.25, and 0.3 the isotropic fluid undergoes a transition to an orientationally ordered fluid at high density. For $\kappa=0$ and $\kappa=0.25$ the fluid is strongly ferroelectric. For $\kappa=0.3$, however, the simulations show that the fluid has no preference for ferroelectric order over antiferroelectric order. This implies that the free energies of the ferroelectric and antiferroelectric phases must be very similar at this dipole separation.

An accurate theoretical calculation of the free energy of such dense fluids is, at present, unfeasible. In view of this we shall estimate the relative free energies of the ferroelectric and antiferroelectric states of a lattice of dipolar hard spheres and show that the stable polarization state changes with the dipole separation.

Tao and Sun [16] have shown that the ground state close-packed crystal structure of regular dipolar hard spheres ($\kappa=0$) in the ferroelectric state is body-centered tetragonal (BCT) with lattice vectors $a_0\hat{\mathbf{x}}$, $b_0\hat{\mathbf{y}}$, and $c_0\hat{\mathbf{z}}$ and cell parameters

$$a_0=\sigma\sqrt{3/2}, \quad b_0=\sigma\sqrt{3/2}, \quad c_0=\sigma. \tag{5}$$

The close-packed reduced density is $\rho_0^*=4/3$. We assume that BCT is the stable state at finite temperature for both ferroelectric and antiferroelectric phases. This assumption will be sufficient to show that a ferroelectric-antiferroelectric crossover can be driven by dipolar interactions alone and without an accompanying structural transition. The BCT structure can be considered as a lattice of chains, each comprised of spheres in contact, aligned along the z direction. Chains are a structural motif found in fluid and solid phases of dipolar hard spheres [4,17]. For densities $\rho<\rho_0$ we choose cell parameters

$$a=\gamma a_0, \quad b=\gamma b_0, \quad c=\sigma, \tag{6}$$

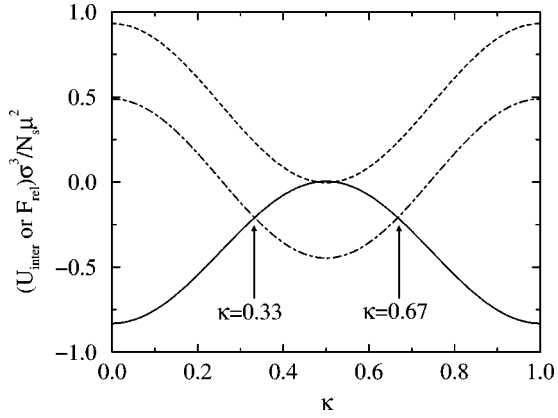

FIG. 6. Interchain energies U_{inter} and relative free energies F_{rel} for the ferroelectric (f) and antiferroelectric (a) body-centered tetragonal lattices as a function of κ, with reduced dipole moment $\mu^*=1.25$ and reduced density $\rho^*=0.925$: $U^f_{\text{inter}}=F^f_{\text{rel}}$ (solid line); U^a_{inter} (dashed line); F^a_{rel} (dot-dashed line).

where $\gamma=\sqrt{\rho_0/\rho}$, so that the spheres in a given chain remain in contact. This reflects the fact that the expansion of a real close-packed lattice would likely be anisotropic by virtue of the strong intrachain interactions.

Consider a sphere, on a given chain, with coordinates (0,0,0). Spheres in that chain have coordinates $(0,0,\pm j\sigma)$ where $j=0,1,2,\ldots$. The dipoles on each sphere on a given chain are aligned parallel to the chain. Spheres in the four nearest-neighboring chains have coordinates $(\pm a/2,\pm b/2, \pm(j+1/2)\sigma)$. Spheres in the four next-nearest-neighboring chains have coordinates $(\pm a,0,\pm j\sigma)$ and $(0,\pm b,\pm j\sigma)$. Tao and Sun evaluated the contribution of chain-chain interactions beyond next-nearest neighbors to be $\sim$1% [16] and so we shall ignore these here. In the antiferroelectric phase the four nearest neighbors of a given chain are aligned antiparallel to it, while the four next-nearest neighbors are aligned parallel to it. We take the polarization in the ferroelectric phase to be $P=1$, i.e., all chains are aligned parallel to one another. We have computed the energies of the ferroelectric and antiferroelectric states, U^f and U^a, respectively, as a function of κ. All dipole-dipole interactions between spheres with $|j_1-j_2|=0,1,2,\ldots,10^5$ were included, which is sufficiently long ranged for our purposes. The interactions between dipoles on the same sphere were not included in the energy sum. We estimate the free energies of the ferroelectric and antiferroelectric states by including the orientational entropy due to the presence of ''up'' and ''down'' dipoles, i.e.,

$$F^f=F_0+U^f_{\text{intra}}+U^f_{\text{inter}}, \tag{7}$$

$$F^a=F_0+U^a_{\text{intra}}+U^a_{\text{inter}}-N_s k_B T\ln 2. \tag{8}$$

F^f and F^a are the free energies of the ferroelectric and antiferroelectric phases, respectively, U_{intra} and U_{inter} are the intrachain and interchain energies, respectively, and F_0 contains other contributions to the free energy which are assumed to be equal in both phases.

Since the intrachain energy is identical in the ferroelectric and antiferroelectric phases, the relative free energy, $F_{\text{rel}}=(F-F_0-U_{\text{intra}})$, is sufficient to identify the thermody-

TABLE II. Energies for the ferroelectric and antiferroelectric body-centered tetragonal lattices with dipole separation $\kappa\sigma$ and reduced density ρ^*. U_{intra} is the intrachain energy and U_{inter} is the interchain energy.

κ	ρ^*	$U_{\text{intra}}\sigma^3/N_s\mu^2$	$U_{\text{inter}}\sigma^3/N_s\mu^2$	
			Ferroelectric	Antiferroelectric
0.25	0.9	−11.4385	−0.3799	0.4236
0.30	0.9	−12.4416	−0.2622	0.2924
0.30	0.925	−12.4416	−0.2882	0.3228

namically stable state. Figure 6 shows U_{inter} and F_{rel} as a function of κ for the two polarization states with $\mu^*=1.25$ and $\rho^*=0.925$. With this dipole strength and density the antiferroelectric phase is seen to be more stable than the ferroelectric phase at dipole separations in the range $0.33\sigma \leqslant \kappa\sigma \leqslant 0.67\sigma$. The variation in energy in the two states is due to the change in proximity of dipoles in neighboring chains, which is itself dictated by the underlying BCT structure. With $\mu^*=1.25$ and $\rho^*=0.9$ the corresponding range of dipole separations is $0.32\sigma \leqslant \kappa\sigma \leqslant 0.68\sigma$.

In Table II are shown the intrachain and interchain contributions to the configurational energy for $\kappa=0.25$ and $\rho^*=0.9$, and for $\kappa=0.3$ and $\rho^*=0.9,0.925$. The lattice configurational energies are 20–30 % higher than those from fluid simulations with the same parameters, which is to be expected. In the lattice calculations the magnitude of the interchain energy is only 2–4 % that of the total energy. In the ferroelectric phase the interchain energy is negative, corresponding to attractions between chains, while in the antiferroelectric phase the chain-chain interactions are repulsive. Therefore, the antiferroelectric phase becomes more stable when its orientational entropy compensates for the difference in interchain energy between the two polarization states.

From our simulations with $\mu^*=1.25$ and $\rho^*=0.9,0.925$ it appears that the antiferroelectric phase is at least as stable as the ferroelectric phase for dipole separations $\kappa\sigma \geqslant 0.3$. An upper limit on $\kappa\sigma$ could not be determined using simulations due to the convergence difficulties highlighted in Sec. III C. There is, however, good agreement between the lower limit on $\kappa\sigma$ obtained from the simulations of the fluid and that predicted by the lattice calculations.

V. CONCLUSION

In this paper we have discussed a variation of the dipolar hard-sphere model, where each sphere carries two dipoles displaced towards the edges. We have presented simulation results for a fixed dipole moment $\mu^*=1.25$ and densities in the range $0.4 \leqslant \rho^* \leqslant 0.925$. For dipole separations $\kappa\sigma=0$, 0.25σ and 0.3σ we observe transitions from the isotropic fluid to orientationally ordered phases as the density is increased. For $\kappa=0$ and 0.25 the high-density fluids have net polarization and so they are ferroelectric fluids. For $\kappa=0.3$, however, the high-density fluid has no strong preference for ferroelectric order over antiferroelectric order. In a sense the antiferroelectric fluid can be termed a normal nematic fluid by virtue of its $\hat{\mathbf{n}} \leftrightarrow -\hat{\mathbf{n}}$ symmetry, where $\hat{\mathbf{n}}$ is the preferred direction of alignment. The simulation results indicate that the antiferroelectric fluid becomes at least as stable as the ferroelectric fluid when $\kappa=0.3$ and $\rho^* \geqslant 0.9$. To gain some insight into this effect we have performed an elementary lattice calculation which shows that the antiferroelectric phase is thermodynamically stable over a range of dipole separations. Furthermore, the predicted range of stability is consistent with the simulation results. This is an example of a fluid in which dipole-driven orientational order occurs without a net polarization.

ACKNOWLEDGMENTS

The financial support of the National Science and Engineering Research Council of Canada is gratefully acknowledged. P.J.C. would like to thank the Killam Foundation of the University of British Columbia for financial support.

[1] M. Born, Sitzungsber. K. Preuss. Akad. Wiss., Phys. Math. K1. **25**, 614 (1916); Ann. Phys. (Leipzig) **55**, 221 (1918).
[2] D. Wei and G. N. Patey, Phys. Rev. Lett. **68**, 2043 (1992); Phys. Rev. A **46**, 7783 (1992).
[3] J. J. Weis and D. Levesque, Phys. Rev. E **48**, 3728 (1993).
[4] D. Levesque and J. J. Weis, Phys. Rev. E **49**, 5131 (1994).
[5] D. Wei, G. N. Patey, and A. Perera, Phys. Rev. E **47**, 506 (1993).
[6] B. Groh and S. Dietrich, Phys. Rev. Lett. **72**, 2422 (1994); **74**, 2617 (1995); Phys. Rev. E **50**, 3814 (1994).
[7] G. Ayton and G. N. Patey, Phys. Rev. Lett. **76**, 239 (1996); Phys. Rev. E **55**, 447 (1997).
[8] R. E. Rosensweig, *Ferrohydrodynamics* (Cambridge University Press, Cambridge, England, 1985).
[9] E. Blums, A. Cebers, and M. M. Maiorov, *Magnetic Fluids* (de Gruyter, New York, 1997).
[10] G. Ayton, M. J. P. Gingras, and G. N. Patey, Phys. Rev. E **56**, 562 (1997), and references therein.
[11] S. W. de Leeuw, J. W. Perram, and E. R. Smith, Proc. R. Soc. London, Ser. A **373**, 27 (1980).
[12] D. J. Adams and I. R. McDonald, Mol. Phys. **32**, 931 (1976).
[13] C. Zannoni, in *The Molecular Physics of Liquid Crystals*, edited by G. R. Luckhurst and G. W. Gray (Academic Press, New York, 1979), Chap. 3, pp. 191–220.
[14] P. G. de Gennes, *The Physics of Liquid Crystals* (Clarendon Press, Oxford, 1974).
[15] R. Eppenga and D. Frenkel, Mol. Phys. **52**, 1303 (1984).
[16] R. Tao and J. M. Sun, Phys. Rev. Lett. **67**, 398 (1991).
[17] J. J. Weis and D. Levesque, Phys. Rev. Lett. **71**, 2729 (1993).